An Innovative Integrated Framework for Cooperative Search and Track of Moving Emitters in Areas with Obstacles

Samine Karimi and Fariborz Saghafi*
Department of Aerospace Engineering, Sharif University of Technology, Tehran, Iran

***Abstract*—In this paper, the problem of detection and tracking of emitters by multiple flying-vehicles, working in a cooperative manner, is considered. The radio sensor on each vehicle is capable of measuring the distance of the vehicle to the radio emitter. The goal is to detect the presence of such emitters, localize, and then track them. Meanwhile, the emitter can be moving or stationary, and may go beyond some environmental obstacles that prevent it from being sensed. The proposed procedure optimizes the routes and tasks of the employed flying-vehicles by minimizing a suitably-defined cost function. Moreover, the appropriateness level of the assigned routes and tasks is continuously assessed, so that if it drops below an acceptable threshold due to the dynamics of the scenario, optimization is performed again and the routes and tasks are renewed. The simulations, as well as the complexity discussion, verify effectiveness of the proposed method, considering the applied requirements and limitations.**

***Index Terms*—Radio intercept, Distributed cooperative search, Task and route optimization, Range sensor, Environmental obstacles.**

NOMENCLATURE

R_c	maximum communication range of vehicle
R_s	maximum radio sensing range of vehicle
Υ	unawareness value
Υ_J	joint unawareness value
P_r	received signal's power
d	distance
$\mathcal{L}$	likelihood value
$\mathcal{L}_J$	joint likelihood value
μ	mean value of distribution
σ	standard deviation of distribution
θ_{HP}	antenna's half-power beamwidth
ΔT	sampling interval
$\mathbb{E}\{\cdot\}$	expectation notation
$\Delta\mathcal{J}^k$	term of cost function for k'th step
$\mathcal{J}$	total cost function
N_{V}	number of vehicles
N_T	number of detected emitters
$R_{min.}$	minimum turning radius
$V_{\infty R_{min.}}$	velocity related to minimum turning radius
$n_{R_{min.}}$	load factor related to minimum turning radius
g	gravity acceleration
$\mathbf{V}_B^I$	velocity vector
$\mathbf{\Omega}^{BE}$	skew symmetric matrix of the angular velocity vector of vehicle w.r.t. the earth
$\mathbf{s}_{BE}$	displacement vector of the vehicle w.r.t. the earth
m_v	vehicle's mass
$f_{a,p}$	aeropropulsive (aerodynamic and propulsive) force
f_g	gravity force
$\propto$	proportional to

1 INTRODUCTION

The cooperative intelligence concept has been widely studied in recent works [1], [2].

Many researches have been carried out to prove the advantageous of cooperation in different missions, for example, search and rescue (SAR) by a team of multiple agents [3] or multiple multicopters [4], cooperative localization [5], surveillance [6], tracking [7], search and attack [8], and animal monitoring [9].

Considerable works have been done specifically on the subject of cooperative search with different simplifications. For instance, in [10], the idea of using a map for measuring the suitability of search, and a map for measuring the tracking error is suggested. In this work, each vehicle uses multiple sensors (besides a range detector) so that the objects' positions are supposed to be known whenever they locate in the vehicle's field of view. Therefore, no detection scheme is defined. Similar notes can be argued about [11] where the seeker installed on the vehicles measures both range and direction of emitters, or about [12] where the vehicles are equipped with optical camera sensors. Moreover, the problem of searching for only one emitter by multiple vehicles is considered in [13]–[15].

In the present paper, the main goal is to develop a methodology for searching a region of interest for possible radio emitters, and then tracking them. These emitters can appear and disappear from the region at any time. So, the vehicles should simultaneously search for undetected emitters and track the detected ones. As explained before, this procedure can be efficiently done through the cooperation of the agents. The cooperative procedure is done in a distributed manner, such that the vehicles communicate and share information with each other. In addition, cooperative search is studied in the context of radio emitters as targets of interest, and flying-vehicles as agents. Flying-vehicles are commonly used in different missions for their lower cost and weight and their human safety [16], [17]. In details, it is noteworthy that the communication range of each vehicle is limited, so that each vehicle can communicate only with its neighboring

vehicles. Each vehicle moves on trajectories that are generated by running a route optimization at each step. This optimization is performed independently of other vehicles, based on the information collected by that vehicle and its neighbors. Moreover, as our vehicle is a flying-vehicle, there are limits on the weight and expense of the sensors mounted on it. Therefore, we have assumed a common case, that each flying-vehicle has only an RSSI (Received Signal Strength Indicator) sensor to measure the emitter's range. Obviously, an object cannot be localized solely by finding its range. But, it can be detected with the help of other vehicles' information, or intercepting its signal for a period of time. In this regard, a detection scheme is defined, based on the emitters' ranges sensed by the vehicles. In addition, the criteria for search and track schemes are well-formulated, according to the received signal power at the vehicle's receiver and the characteristics of the employed tracking filter.

In summary, the contributions of this paper is highlighted as:

- Our solution to the surveillance problem benefits from using light and cost effective flying-vehicles, since they are equipped with only range sensors.
- Considering the problem such that the vehicles have cooperation through communications with each other makes the solution more complicated. But this fact results in improved success rate of the mission.
- Solving the surveillance problem for multiple emitters, which can be moving or stationary, and can appear and disappear from the region at any moment, is another privilege of the proposed method.
- An efficient innovative algorithm is developed for performing a mission with the goal of searching for and localizing undetected emitters, while tracking the detected ones, simultaneously.
- The proposed algorithm considers the problem of obstacles (e.g., mountains) in the surveillance regions, which prevent the vehicles from sensing the radio signal of an emitter behind the obstacle.

In the following, the cooperative surveillance problem is presented in Section 2, where the solution is also proposed. Next, in Section 3, the simulation results of performing the proposed optimization for some scenarios are presented. Section 4 discusses the complexity of the proposed algorithm. Finally, the paper is concluded in Section 5.

2 Cooperative search

A known number of flying-vehicles is performing cooperative search in a predefined region of interest to find an unknown number of moving or fixed radio emitters. They roam in the region to intercept any possible signal. All the vehicles fly at similar constant height level. Each vehicle is equipped with only a common, low cost, RSSI sensor to measure the emitter's distance to the vehicle. Emitters are mobile, so they may leave or enter the search region causing the signals appear or disappear. However, when an emitter is detected, only one vehicle will track it. Each vehicle is capable of performing only one of the tasks as defined below at a moment:

- search: when the vehicle is searching the region, its receive antenna is omnidirectional, intercepting the possible signals from all 360° around the vehicle.
- track: when a vehicle is assigned to track an emitter, it constantly estimates the position of the emitter and tries to narrow its intercepting beam towards the estimation point, so that it receives only the tracked emitter's signal, but with higher SNR (Signal to Noise Ratio) and accuracy. In this way, a detected emitter's state (position, velocity, and acceleration) is monitored continuously.

Meanwhile, the vehicles share their information with their neighbors within the maximum communication range of R_c. They, also, have a maximum radio sensing range R_s, as shown in Fig. 1.

The surveillance region, containing the vehicles and emitters, is assumed two-dimensional, and the vehicles and emitters are considered point masses in this region. Moreover, there may be some obstacles (e.g., natural barriers or mountains) which prevent the vehicles from receiving signal from the emitters. Thus, the covered emitters can be detected only when they get LOS (Line Of Sight) with a vehicle, as a result of the vehicles searching or emitters' movements. It is assumed that the obstacles' map is available for all vehicles during the mission. As a general guideline, a mission having more accurate detections and efficient tracking of the detected emitters in less time duration, is desired.

In order to search the region of interest, each vehicle plans its path and task (search or track) through a constrained optimization procedure. In each optimization run (namely, an optimization phase), the route of each vehicle is determined for the next multiple steps. In other words, each optimization phase consists of multiple time steps, in which, the optimization is performed to determine the path of the vehicle during the steps of that phase. To do so, a gridding network is proposed for defining the paths (or equivalently the steps). To obtain the cost function of such optimization, three criteria are evaluated over the region for each vehicle, as illustrated in the following.

2.1 Environmental unawareness criterion

In order to define the environmental unawareness criterion, each point in the region is assigned an unawareness value which represents the amount of vehicle's unawareness from that point. This value can be obtained by considering the fact that further points have more unawareness values. Accordingly, each point's unawareness value (Υ) can be obtained from:

$$\Upsilon \propto \begin{cases} \frac{1}{P_r} \propto d^4 & \text{if there is no obstacle in between,} \\ \infty & \text{if there is an obstacle in between,} \\ 0 & \text{if the point is located on an obstacle.} \end{cases} \tag{1}$$

where Υ represents the unawareness value, P_r is the received signal's power, d is the distance between the specified point and the vehicle, and the 4 power comes from the traditional radar equation. This means that for the points behind obstacles,

where radio emitters have no LOS* to a vehicle's sensor, we have complete unawareness. Also, note that for the points on the obstacles, we have complete awareness, i.e., zero unawareness, as it is assumed that we are looking for the free space emitters in the region. Assuming that (x_0, y_0) and (x, y) are the position coordinates of a vehicle and an arbitrary point in the search region, respectively. The unawareness value is then calculated as presented in Equation (2).

$$\Upsilon(x, y) = k\left((x - x_0)^2 + (y - y_0)^2\right)^2. \tag{2}$$

Figure 2 shows a sample of region's unawareness values, in which one vehicle is located at $(0, 0)$, and there are three rectangular obstacles. As can be observed, further points from the vehicle have larger values.

It is noteworthy that the unawareness values of the points over which a vehicle is already passed, are set to zero for a short duration. That means, the vehicle has complete awareness of these points at least for a period of time after passing over them. However, after a while, and as the vehicle goes away, these zero unawareness points will get nonzero values again based on Equation (2). In fact, the unawareness of the vehicle about that points is now returned.

2.2 Emitter likelihood criterion

Normally, the signal emitted by a non-detected emitter is sensed by a search vehicle that has LOS with the emitter. Due to non-idealities and environmental factors, the emitter's range is measured with error. In this respect, the emitter likelihood criterion is defined to allow to detect and localize emitters. In this regard, the points with range distance equal to the measured range are assigned the value of one (which is the maximum likelihood value). Then, the points with other distances are assigned values which decrease in a Gaussian distribution pattern, as we go further from the points with maximum values (one). As an example, it is assumed that a signal from an emitter at $(40, 35)$ is received and detected by a vehicle at $(10, 25)$. The RSSI sensor has measured the distance as $31.6m$.

The assumed Gaussian distribution pattern is shown in Fig. 3. As seen, the points further from the measured emitter range $(31.6m)$ have less probability values obtained from the Gaussian distribution pattern. As mentioned, the central axes of this Gaussian distribution are the points with range equal to the measured range $(31.6m)$ and its variance (σ^2) is assumed to be proportional to the measured range. Intuitively, the reason is that higher measured range is obtained from the weaker signal of a further emitter. In other words, its received signal would have less SNR. Therefore, lesser measurement accuracy is expected, which results in larger variance of that point's distribution. Indeed, each point's likelihood value represents the probability of the emitter's presence at that point, based on the measurements of the sensor. Note that, the likelihood values of the points behind and in the obstacles are set to zero. The reason is that there is no chance to receive a measurement from an emitter with no LOS. The likelihood distribution can be written as

$$\mathcal{L}(d) = \frac{1}{\sigma(\mu)\sqrt{2\pi}} \exp\left(-\frac{(d-\mu)^2}{2\sigma(\mu)^2}\right), \tag{3}$$

where μ is the mean value of the distribution and, as explained before, it is the sensed range measurement. Also, σ^2 is the variance of the distribution and d is the distance of the point for which the likelihood value is calculated. It is noteworthy that, as mentioned before, σ^2 increases as μ increases, because the measurement accuracy decreases for larger distances. To capture this dependency, we have [18]

$$\sigma(\mu) = \frac{\theta_{HP}}{\sqrt{2\pi \mathrm{SNR}}}, \tag{4}$$

where θ_{HP} is the receive antenna's half-power beamwidth that is a sensor characteristic. Also, we can obtain from the radar equation that for a receiver intercepting an emitter at a distance μ

$$\mathrm{SNR} \propto \frac{1}{\mu^2}, \tag{5}$$

and substituting in Equation (4), we have

$$\sigma(\mu) \propto \mu. \tag{6}$$

In other words, a larger sensed range measurement results in an emitter's likelihood function with larger variance.

2.3 Tracking precision criterion

This criterion is defined for the detected emitters, which are being tracked. A point with likelihood value exceeding a predefined threshold, is alarmed as a new emitter and should be tracked. In this regard, the likelihood values of all points are examined: any point with a likelihood value more than the threshold is declared a new detected emitter. As a reasonable case, the threshold is set as a multiple of the mean likelihood value of all points of the region. Subsequently, each detected emitter is assigned a vehicle to be tracked by.

The tracking precision criterion is defined as the detected emitter's tracking error. A suitable tracking filter will be chosen in the subsequent sections and its estimation error will be used for the precision criterion.

2.4 Sharing information with neighbors

At each optimization phase, each vehicle should be assigned one of the two tasks of search or track. Also, a search vehicle evaluates the two criteria values of unawareness and emitter likelihood, for all points of the region. But, a tracking vehicle evaluates only the tracking precision criterion.

After defining and evaluating the aforementioned three criteria for each vehicle, the assessments of the neighboring vehicles from the region should be combined and shared with each other. The neighbors are determined based on the vehicles' communication ranges (R_c). The result of such information sharing about each point of the region, is three values of joint unawareness, joint emitter likelihood, and joint tracking precision. For a group of neighboring vehicles,

*Line Of Sight

the joint unawareness and joint emitter likelihood values are computed by combining the information of those vehicles which are in the search mode. However, the joint tracking precision value is produced only based on the information shared by the neighboring vehicles in the tracking mode. Thus, for a tracking vehicle, the unawareness and emitter likelihood values are produced by combining the corresponding values of that vehicle's neighbors, which are in the search mode. In fact, the vehicles in the track mode, have no effect on the searching procedure. The reason is that the tracking vehicles have no awareness of the areas around them; because they are just tracking their assigned emitters. On the other hand, the tracking precision value for a tracking vehicle is produced based on the information of that vehicle and its neighbors which are in the track mode.

The combining procedure to obtain the aforementioned joint parameters is explained in the following:

2.4.1 Joint unawareness: The joint unawareness value of a point is the minimum of the unawareness values of all N number of search neighbors,

$$\Upsilon_J(x,y) = \min_i \Upsilon_i(x,y) \ , \quad i \in (1,\cdots,N). \tag{7}$$

In fact, low unawareness values for a vehicle in an area indicates well coverage of that area. So, there is no need to force other vehicles to move to that point and cover it again.

2.4.2 Joint emitter likelihood: The emitter likelihood values of searching neighbors should be combined to find the undetected emitters. For this goal, assume that U_i is the i'th receiver's observation from an emitter and also X is the occurrence of that emitter's presence at a certain point of the region $(\mathbf{p}_0)$. The probability of such occurrence, while $\{U_i, i = 1,\cdots,N\}$ are observed, can be obtained according to the Bayesian law [19], as

$$\Pr(X|U_1,\cdots,U_N) = \frac{\Pr(U_1,\cdots,U_N|X)\Pr(X)}{\Pr(U_1,\cdots,U_N)}, \tag{8}$$

which, due to independency of occurrence probabilities U_i and U_j $(i \neq j)$ conditioned on X, can be rewritten as

$$\Pr(X|U_1,\cdots,U_N) = \frac{\prod \Pr(U_i|X)\Pr(X)}{\Pr(U_1,\cdots,U_N)}. \tag{9}$$

For $\Pr(U_i|X)$ one can employ the Bayesian law again:

$$\begin{aligned}\Pr(X|U_1,\cdots,U_N) &= \prod \left(\frac{\Pr(X|U_i)\Pr(U_i)}{\Pr(X)}\right)\frac{\Pr(X)}{\Pr(U_1,\cdots,U_N)} \\ &= \prod \Pr(X|U_i)\frac{\prod \Pr(U_i)}{\Pr(X)^{N-1}\Pr(U_1,\cdots,U_N)} \\ &= k_0 \frac{\prod \Pr(X|U_i)}{\Pr(X)^{N-1}},\end{aligned} \tag{10}$$

where k_0 is constant and independent of X, which means that in evaluating the emitter's likelihood of a point $(\mathbf{p}_0)$, when conditioned on observation $\{U_i, i = 1,\cdots,N\}$, k_0 is constant for all points of the region. On the other hand, since $\Pr(X)$ has a uniform distribution (since there is no information about the presence of the emitter at different points of the region before starting the mission and observing any measurement.), we can write:

$$\Pr(X|U_1,\cdots,U_N) = k \prod \Pr(X|U_i), \tag{11}$$

where k is constant and its value is independent of $\mathbf{p}_0$, which means that it is constant for all points of the region. Therefore, it can be ignored in the thresholding process of the likelihood values for finding emitters.

Furthermore, notice that $\Pr(X|U_i)$ is the probability of the emitter's presence at $\mathbf{p}_0$ conditioned on the i'th receiver's observation, which represents the likelihood value of the i'th vehicle individually. Thus, Equation (11) states that the joint likelihood value of N receivers can be obtained from

$$\mathcal{L}_J(\mathbf{p}_0) = \prod \mathcal{L}_i(\mathbf{p}_0). \tag{12}$$

Considering the joint values of all points of the region, the point, for which the likelihood value is larger than the threshold, is declared as the location of a new emitter.

It is noteworthy that to get better performance, another improvement is considered in producing the joint likelihood value. We can use the information sensed by vehicles in previous times, which is remained in their memories. Indeed, the likelihood values related to an individual vehicle, in different subsequent times, can be combined, similar to the case of combination of values of different vehicles:

$$\Pr(X|U^t, U^{t-1}) \propto \Pr(X|U^t)\Pr(X|U^{t-1})^{\xi}, \tag{13}$$

where t denotes the observation time, and the likelihood value of the previous time (which is between 0 and 1) is powered with a forget factor (ξ), so that the previous time value has less effect than the current value. As a result, as the time goes on, the vehicle forgets the past status, gradually.

2.4.3 Joint tracking precision: Each tracking vehicle has an estimation of the position of the emitter it is tracking. In this paper, the tracking procedure is done using a variant of Kalman filter, namely, the $\alpha\beta\gamma$ filter, in which a good trade-off is met between the low computational burden enforced by the limitations of each vehicle's processor and the tracking accuracy needed in the surveillance missions.

a. $\alpha\beta\gamma$ filter

In order to use the original Kalman filter, detailed dynamic system model is needed, and states' values are estimated in a formal and rigorous manner. Alternatively, one can employ the $\alpha\beta\gamma$ filter which is basically a Kalman filter when the model meets some simple assumptions. The detailed dynamic system model is not needed in the $\alpha\beta\gamma$ filter and it estimates the states in a simple process. This filter presumes that a system is adequately approximated by a model having three internal states, where the first state is obtained by integrating the value of the second state and the second state is obtained by integrating the value of the third state over time. This approximation is adequate for many simple systems, for example, the emitter dynamics in our case, where position and velocity are obtained as the time integral of velocity and acceleration, respectively. In addition, a Kalman filter, which is designed to track a moving object using a constant-acceleration dynamics model with process noise covariance and measurement covariance

held constant (which is our case, in this paper.), converges to the same structure as an $\alpha\beta\gamma$ filter [20].

Two separate $\alpha\beta\gamma$ filters are used in the x and y directions. For both directions the equations are the same. Therefore, in the following, just the equations for x direction is presented.

The equations of this filter are defined in two parts. First for the prediction part we have:

$$\begin{aligned} x_p(k) &= x_s(k-1) + \Delta\mathrm{T} v_s(k-1) + \frac{\Delta\mathrm{T}^2}{2} a_s(k-1), \\ v_p(k) &= v_s(k-1) + \Delta\mathrm{T} a_s(k-1), \\ a_p(k) &= a_s(k-1), \end{aligned} \tag{14}$$

where $\Delta\mathrm{T}$ is the sampling interval, $x_p(k)$, $v_p(k)$ and $a_p(k)$ are the predicted object position, velocity and acceleration at time $k\Delta\mathrm{T}$, respectively, and $x_s(k-1)$, $v_s(k-1)$ and $a_s(k-1)$ are the smoothed object position, velocity, and acceleration at time $(k-1)\Delta\mathrm{T}$, respectively.

For the smoothing part, using the measured position, we have:

$$\begin{aligned} x_s(k) &= x_p(k) + \alpha \left(x_o(k) - x_p(k)\right), \\ v_s(k) &= v_p(k) + \frac{\beta}{\Delta\mathrm{T}} \left(x_o(k) - x_p(k)\right), \\ a_s(k) &= a_p(k) + \frac{2\gamma}{\Delta\mathrm{T}^2} \left(x_o(k) - x_p(k)\right), \end{aligned} \tag{15}$$

where $x_o(k)$ is the measured position (observation) at time $k\Delta\mathrm{T}$, and α, β, and γ are the filter gains.

This filter's estimation error consists of two parts: the steady state error (or the noise error) and the transient error (or the maneuver error). The maneuver error can be computed from [21]:

$$\frac{\Delta\mathrm{T}^2(2-\alpha)}{\alpha\beta(4-2\alpha-\beta)}. \tag{16}$$

As can be observed, this error is a function of only the constant parameters of the filter and is independent of the geometry of the vehicles. Thus, this term has no role in the optimization procedure. The noise error can be obtained as [20]:

$$\begin{aligned} \sigma_P^2 =& \mathbb{E}\left[\left(x_p(k) - x_t(k)\right)^2\right] \\ =& \frac{8\beta^2 + \alpha(4-2\alpha-\beta)(2\alpha\beta - \gamma(2-\alpha))}{(2-\alpha)(4-2\alpha-\beta)(2\alpha\beta-\gamma(2-\alpha))} \sigma(\mu)^2, \end{aligned} \tag{17}$$

where $\mathbb{E}$ denotes the expectation notation, x_t represents the true emitter's position, and $\sigma(\mu)$ can be obtained from Equation (4) for an object at distance of μ.

Regarding the neighbors' tracked emitters, each vehicle considers minimizing the tracking error by considering whether to track the neighbors' dedicated emitters or not. In other words, all neighboring vehicles try to maximize the joint tracking precision of detected emitters by assigning appropriate vehicles to track each emitter.

b. Obtaining position observation from range information

As the tracking $\alpha\beta\gamma$ filter is suitable for a linear model, the object Cartesian coordinates ($\mathbf{p} = [x, y]$) is appropriate for tracking and should be the input to this filter, outcoming from the fact that the object usually moves in a straight line. However, more complicated filters such as extended Kalman filter or unscented Kalman filter [22] should be used for nonlinear models. This means that the polar coordinates ($[r, \theta]$) are not appropriate, and the range only measurement (r) is not sufficient for our means. In this regard, a solution is proposed in the following to obtain the Cartesian coordination of the emitter from the range information available from the sensors, so that the $\alpha\beta\gamma$ filter can be suitably applied.

In order to employ the $\alpha\beta\gamma$ filter, the two Cartesian coordinates of the emitter's position should be determined from the received signal, that only measures just the distance of the emitter (r). To overcome this issue, the locus of two circles, related to the current time and the last time steps, are plotted, using the two different sensor's range measurements as the circles radii and the two different vehicle's positions as the centers of the circles (see Fig. 4). Then, the nearest intersection of these two circles to the predicted point ($\mathbf{p}_p(k) = [x_p(k), y_p(k)]$) is chosen as the Cartesian observation ($\mathbf{p}_o(k) = [x_o(k), y_o(k)]$). It is noteworthy that the step time should be chosen sufficiently small that the emitter's movement is negligible in this duration. In this way, an emitter's position is available each time a range measurement r_k is sensed. Based on this new position, and then using the aforementioned $\alpha\beta\gamma$ filter, the emitter's position can be tracked.

2.5 Optimization problem

For each vehicle the path and task should be determined, such that, considering the whole region and all vehicles, the search and track mission is done suitably. In this way, one can assure that all emitters, present in the region, are detected and tracked as fast and accurate as possible. To do so, an appropriate cost function is defined according to the criteria presented in the previous sections.

2.5.1 Cost function: The cost function of the route/task optimization problem is defined as follows:

$$\begin{aligned} \mathcal{J} &= \sum_{k=1}^{K} \Delta\mathcal{J}^k, \\ \Delta\mathcal{J}^k &= \int\int \Upsilon_J(x,y)dxdy \\ &\quad + \sum_{i=1}^{N_\mathrm{V}} S_i \sum_{m=1}^{N_{\mathcal{L}_\mathrm{max}}} \mathcal{L}_J(x_m, y_m) \times \sqrt{(x_i^\mathrm{V} - x_m)^2 + (y_i^\mathrm{V} - y_m)^2} \\ &\quad + \sum_{i=1}^{N_\mathrm{V}} \sum_{j=1}^{N_T} T_i^j \times (\sigma_P^2)_{ij}. \end{aligned} \tag{18}$$

where $\Delta\mathcal{J}^k$ is the term of cost function for k'th step (i.e., at time $t = k\Delta\mathrm{T}$), K is the number of steps in each optimization run, $\Upsilon_J(x, y)$ is the joint unawareness at point (x, y), and S_i indicates whether this vehicle is searching ($S_i = 1$) or not ($S_i = 0$). Indeed, the first term is the integral of the unawareness values over the whole region of interest during one step. In the second term, $N_{\mathcal{L}_\mathrm{max}}$ and $\mathcal{L}_J(x_m, y_m)$ are the total number of local maximums of the joint likelihood function and their corresponding values, respectively. In addition, $[x_i^\mathrm{V}, y_i^\mathrm{V}]$ is the i'th vehicle's position. The second term is defined such that the vehicles move toward the points that are

more likely of an emitter's presence. In the third term, $(\sigma_P^2)_{ij}$ is the estimation error of tracking the j'th emitter by the i'th vehicle, and T_i^j indicates whether this vehicle is tracking the j'th emitter ($T_i^j = 1$) or not ($T_i^j = 0$). Finally, N_{V} and N_T are the number of neighboring vehicles and detected emitters being tracked, respectively. Minimizing this term aims to track emitters with least estimation error.

In order to perform the optimization, feasible routes should be considered. For this goal a gridding network is assumed, in which the vehicles travel by crossing only to the adjacent nodes in each movement. For illustration, five candidates of feasible routes are shown in Fig. 5, where the current vehicle's position is denoted by number one.

In this paper, GA (Genetic Algorithm) is employed for solving the optimization problem. The GA is a searching process based on the laws of natural selection and genetics.

2.5.2 Optimization constraints: The constraints of the optimization problem are as follows.

1) Task assignment,
$$S_i + T_i = 1, \tag{19}$$
which means that the i'th vehicle is assigned whether to search the region $(S_i = 1, T_i = 0)$ or track an emitter $(S_i = 0, T_i = 1)$.
2) Track assignment,
$$\sum_{j=1}^{N_T} \eta_j = \min(N_T, N_{\mathrm{V}}), \tag{20}$$
which means that a detected emitter should be tracked by only one vehicle (and not more) and also should not be released (if there is any vehicle ready for tracking). In constraint of Equation (20), η_j indicates whether the j'th emitter is being tracked ($\eta_j = 1$) or not ($\eta_j = 0$), and N_T and N_{V} are the number of detected emitters and vehicles, respectively.
3) Vehicle's dynamics,
$$\begin{aligned} &V_v(t) = \frac{ds}{dt}, \\ &V_{v\min.} < V_v(t) < V_{v\max}, \end{aligned} \tag{21}$$
where $V_v(t)$ is the velocity as a function of time, ds is the distance differentiation, and dt is the time differentiation. This means that the velocity limitations of the vehicles are considered besides the equation of motion. In addition,
$$R_{min.} < R(t), \tag{22}$$
which states the constraint on turning radius of the vehicle $(R(t))$. The minimum turning radius of vehicles, according to flying-vehicle's characteristics, can be calculated as [23]:
$$R_{min.} = \frac{{V_\infty}^2_{R_{min.}}}{g\sqrt{n^2_{R_{min.}} - 1}}, \tag{23}$$
where g is the gravity acceleration, and $V_{\infty R_{min.}}$ and $n_{R_{min.}}$ are the velocity and load factor related to minimum turning radius, respectively.
4) Gridding,
$$d_N \approx 4.8 R_{min.}, \tag{24}$$
where (d_N) is the horizontal (or equivalently vertical) distance of the nodes. To illustrate this constraint, suppose that in an extreme scenario the vehicle moves in a sequence of Node 3 to Node 1 to Node 2 to Node 4 as shown in Fig. 6, where the maximum change in the vehicle's heading angle occurs. Near Node 1 and Node 2, this change equals 135 degrees.
Thus, the minimum acceptable distance of two nodes can be obtained from
$$\ell = \frac{d_N}{2} = \frac{R_{min.}}{\tan(45°/2)} \Rightarrow d_N = 4.8 R_{min.}. \tag{25}$$
5) Sensor range.
Two vehicles are assumed neighbors and therefore can share their information only when they are in the communication range of each other:
$$\sqrt{(x_i - x_j)^2 + (y_i - y_j)^2} < R_c, \tag{26}$$
where $[x_i, y_i]$ and $[x_j, y_j]$ are the vehicles positions.
In addition, the vehicle is able to sense a signal from an emitter only if their distance is less than the vehicle's defined sensor range:
$$\sqrt{(x_s - x_t)^2 + (y_s - y_t)^2} < R_s. \tag{27}$$
6) Obstacles.
When obstacles are present in the region, to avoid obstacle collision, only those routes that do not touch the obstacles are accepted. In more details, each of the obstacles in the search area includes some nodes of the preassumed gridding network. Accordingly, these nodes are omitted from the allowable nodes that form a candidate route. For Example, in Fig. 7, there are three rectangular obstacles that the vehicles should avoid colliding with.
Moreover, it is possible that an emitter goes behind an obstacle such that the vehicle has no LOS to that emitter. Therefore, an emitter affects a vehicle's likelihood function only when there is LOS between the emitter and vehicle. To formulate this constraint, it is assumed that the obstacle $\mathbf{B}$ is defined as a set of boundary line segments[†]:
$$\mathbf{B} = \{\ell_i | i = 1, \cdots, L\}. \tag{28}$$
where each line segment (ℓ_i) is considered straight, and L is the number of these segments constituting the obstacle $\mathbf{B}$. Therefore, to have LOS, a line connecting the vehicle to the emitter $(\ell_{LOS}^{\mathrm{vt}})$ should not collide with

[†]Note the 2D consideration, as explained before.

any member of the set $\mathbf{B}$:

$$\mathbf{B} \dashv \{\ell^{\mathrm{vt}}_{LOS}\} = \varnothing, \tag{29}$$

where the $\dashv$ symbol denotes the set of points obtained from the intersection of the lines of the two sets.

Finally, it is obvious that only a vehicle, that has LOS with a detected emitter inside its sensor range, is allowed to be assigned to track that emitter.

2.6 Assessment stage

In order to decrease the computational burden, the cost function is optimized once after multiple step times (instead of at each step time), determining the route for multiple step times. However, when moving through the planned route, the vehicle may experience degraded performance, as the emitters and environmental situations change dynamically. In this regard, at the beginning of each step time, the appropriateness of the planned route and task is evaluated by each vehicle. This evaluation determines whether the planned path and task are still suitable or not. For this purpose, the cost function of Equation (18) is evaluated for the rest of the vehicle's path (i.e., that part of the path that the vehicle has passed is omitted from the summation of Equation (18)):

$$\mathcal{J}_i = \sum_{k=k_t}^{K} \Delta\mathcal{J}_i^k,$$

where k_t is the current step's index. Obviously, the path's cost may vary during the vehicle's travel, as the emitters are moving and new measurements are sensed. In this regard, if the cost of the rest of the path has increased unacceptably, a new planning optimization is performed for that vehicle and the previous one is neglected.

The proposed surveillance scheme is summarized in **Algorithm 1**.

3 Simulation results

In the following, each optimization is performed to obtain the routes for three time steps ($K = 3$ in Equation (18)). Specifically, the genetic algorithm employs the scattered crossover method with a crossover fraction of 0.8. Besides, the Gaussian mutation is utilized for producing the next generations, while the stochastic universal sampling (SUS) technique is applied for the selection procedure [24]. Maximum number of iterations before the algorithm halts is chosen as forty.

The recent six positions of the vehicles are assumed to have zero unawareness values, as illustrated in Section 2.1. If the value of a point's likelihood gets 1,000 times larger than the average of all the values of the region, then that point would be declared as a new emitter. In addition, the vehicles' range sensor is assumed to have a detection range of $170km$, and the vehicles have low frequency communication links, which allow them to be connected with each other through the whole region. Indeed, the obstacles that prevent the radio emitter's signal from being intercepted by the vehicle's range sensor, are not considered barrier for the communication signal. Moreover, each vehicle flies with the velocity of between $120km$ and $180km$ per hour. Thus, setting the load

Algorithm 1 : Algorithm for the cooperative surveillance problem of a group of neighboring vehicles

Require: Set of tasks, locations, and sensor measurements of the vehicles at the current time, i.e., $\{S_i, T_i\}, \{(x_i^{\mathrm{V}}, y_i^{\mathrm{V}})\}, \{R_i\}$ for $i = 1, \cdots, vehiclesNumber$.

Ensure: A solution set of paths and tasks for $i = 1, \cdots, N_{\mathrm{V}}$, Possible new emitters.

a: Solve the constrained optimization problem of finding the best (with the minimum cost) set of paths and tasks among all feasible candidate sets, using the Genetics algorithm.

b: The cost of a candidate set of paths (including K steps) and a candidate set of tasks for the vehicles is calculated as below (lines 1 to 27).

1: Set $i = 0$;
2: **repeat**
3: $i := i + 1$;
4: **if** vehicle$(i) \in$ {Search vehicles} **then**
5: **for** all $(x, y) \in$ region of interest **do**
6: Compute the unawareness value $\Upsilon_i(x, y)$ (Equation 2)
7: Compute the likelihood value $\mathcal{L}_i(x, y)$ (Equation 3)
8: Combine the likelihood values of subsequent times according to Equation 13
9: **end for**
10: **else if** vehicle$(i) \in$ {Track vehicles} **then**
11: Estimate the assigned emitter's position (Equation 15)
12: **end if**
13: **until** $i \leq N_{\mathrm{V}}$
14: **for** all $(x, y) \in$ {region of interest} **do**
15: Compute the joint unawareness $\Upsilon(x, y)$ (Equation 7)
16: Compute the joint likelihood value $\mathcal{L}_J$ (Equation 12)
17: **if** $\mathcal{L}_J > LikelihoodThreshold$ **then**
18: A new emitter is declared detected at (x, y)
19: **end if**
20: **end for**
21: **for all** detected emitters **do**
22: Compute the joint tracking precision σ_P^2 (Equation 17)
23: **end for**
24: Set $k = 0$;
25: **repeat**
26: $k := k + 1$;
27: Compute cost of k'th step $(\Delta\mathcal{J}^k)$ according to Equation 18
28: **until** $k \leq K$
29: Compute $\mathcal{J} = \sum_{k=1}^{K} \Delta\mathcal{J}^k$.
30: Output $\mathcal{J}$

factor as $n_{R_{\min}}$ = 1.8 leads to the minimum turning radius of the vehicles as $R_{\min}$ = 75.7m (from Equation (23)). The distance of nodes is chosen d_N = 380m to meet the constraint of Equation (24). Having a velocity controller, each vehicle goes from a node to its adjacent node in a step time (ΔT). By choosing ΔT = 11s, the velocity of the vehicle remains in the aforementioned bounds. Accordingly, the velocity in longitudinal and lateral directions would be $34.55m/s$, which is more than the minimum allowable speed. Besides, the velocity for passing in the diagonal nodes would be $48.85m/s$ which satisfies the maximum allowable speed. In addition, for satisfying the turning radius constraint, no vehicle can turn back, or remain at its last node. Furthermore, the region of interest, with the dimensions of $19km \times 19km$, is divided to 50 equi-distance nodes. In the following, the distance, time, and velocity values are normalized by d_N = 380m (distance of two adjacent nodes), ΔT = 11s, and $380/11\frac{m}{s}$, respectively. Finally, values of α = 0.5, β = 0.1, γ = 0.001 are used for the tracking filter.

3.1 An instructive scenario

In the following, the ideas mentioned before for optimizing the vehicles' routes and tasks are illustrated by an example.

In this scenario, three vehicles at $(10;5)$ (first vehicle), $(10;30)$ (second vehicle), and $(10;55)$ (third vehicle) are considered. In addition, two emitters, initially at $(41;50)$ and $(35;22)$, are moving with constant velocities of $(0.1;0)$ and $(0;-0.17)$, respectively. Also, three obstacles (for example, mountains) are present in the region of interest, whose boundaries are distinguished by light blue lines in the following figures.

Figure 8 shows the joint likelihood function for the 14'th optimization. In this step, the value of the peak at $(19;19)$ exceeds the threshold, and therefore, a new emitter is declared. From now, two vehicles search the region and the other one tracks the only detected emitter. As expected, since the second vehicle is closer to the detected emitter, it is assigned to track and the other two vehicles continue searching.

As the searching vehicles continue searching, the likelihood function, gradually tends to yield narrower peak until the peak exceeds the threshold in the 34'th optimization and a new emitter at $(23;53)$ is declared. The likelihood values are shown in Fig. 9. Based on the constraint of Equation (20), from now, two vehicles are assigned to track.

The overall vehicles' trajectories are shown in Fig. 10.

It is worth noting that after the second emitter detection, the two tracking vehicles plan their routes only based on the error estimation criterion. The position estimation errors of the two detected emitters are presented in figures 11 and 12. Although some little temporary increase in the x-coordination error is observed at about step#100 due to the vehicle's maneuver, the results show satisfactory convergence.

3.2 Performance evaluation

In this part, the effectiveness of the cooperation between vehicles in the surveillance scenario is investigated.

3.2.1 Effect on detection: First, one stationary emitter is positioned randomly in the region of interest with no obstacle, and a cooperative search mission is performed according to the proposed algorithm. This scenario is repeated for different number of employed vehicles. In fact, each scenario is repeated for 100 times with 100 randomly chosen positions for the emitter, and the mean detection time, is measured. The results are depicted in Fig. 13, where the efficiency of the cooperation in decreasing the mean detection time is obvious. The results suggest that in a cooperative surveillance, increasing the number of search vehicles, initially, has a significant impact on the detection. But, gradually this improvement tends to saturation, which implies that no considerable decrease occurs in the detection time by increasing the number of vehicles, and three is adequate. Moreover, it is observed that one vehicle alone has relatively weak detection performance due to the nature of its range only sensor.

The same result is observed in Fig. 13 for one moving emitter in the region, where 100 random positions are produced for the emitter and the emitter starts to move to the center with a constant velocity of $34.5m/s$. Also, notice that so long as the emitter's speed is not very high w.r.t. the step time, such that it satisfies the constraint of Section 2.4.3, introduced for the intersection localization method, the algorithm well detects the emitter and there is not significant difference between a moving emitter and a stationary emitter from the detection time point of view.

3.2.2 Effect on coverage: In this part, the effect of vehicles' number on the coverage level of the region is examined. In fact, for different number of vehicles, the previously mentioned region of interest without any emitter or obstacle is considered. In this case, according to what stated in Section 2, only the unawareness criterion determines the vehicles' routes, and the values of other two terms are zero. The value of the resulted cost function, which is indeed the joint unawareness level, is depicted in Fig. 14 over 20 optimization phases for 1 to 3 vehicles.

First, notice that the unawareness values are less for more vehicles. In addition, it is worth noting that in addition to the decreasing behavior of the unawareness over the 20 phases, each case converges to a final value which, also, decreases by adding more vehicles. Indeed, for a limited number of vehicles searching a region of interest, the proposed optimization scheme, finally, leads to optimum locations for the vehicles, where the vehicles have the most awareness of the region by roaming at. Moreover, similar to the previous analysis (Fig. 13), one vehicle (without cooperation) has relatively weak performance as a result of using range only sensor.

3.2.3 Effect of emitter's velocity: The effect of emitter's velocity on the tracking performance is examined. To do so, two vehicles and one emitter are considered. Indeed, regarding the previous analyses' results, it can be observed that two vehicles are sufficient for such mission. The vehicles are positioned initially at the two corners of $(1;1)$ and $(1;59)$. In six different scenarios, the emitter starts from $(40;55)$ with a velocity chosen from Table I.

The resulted vehicles' trajectories, upto the 43'th optimization, are shown in Fig. 15.

The mean error of the emitter's position estimation in the phase of stable tracking is shown in Fig. 16. As can be observed, it increases with the increasing of the emitter's velocity.

The reason lies in the fact that in producing the position measurement of the emitters by the intersection method presented in Section 2.4.3, there was an assumption of emitter's being approximately stationary w.r.t. the vehicle in two successive steps, as mentioned before. However, by increasing the emitter's velocity, this assumption gets more violated. Moreover, it can be inferred from the results that localization of a stationary emitter is performed perfectly due to the feature of intersection method.

3.3 Validation with regard to recent works

In this part, the efficiency of the proposed search algorithm is compared with two similar recent works of the same field.

First, the search algorithm of [25] is considered. In this article, the flying-vehicles' paths are determined using a distributed ant colony optimization (ACO) algorithm. Assume a $50km \times 50km$ region with $1,000 \times 1,000$ nodes. Two vehicles with the initial locations of $(0,0)km$ and $(50,0)km$ are to search the region for eight stationary emitters, as in Fig. 17. The vehicles have the speed of $250\frac{m}{s}$ with the minimum turning radius of $100m$. In this regard, the distance of two adjacent nodes is chosen $500m$ to satisfy Equation (25). As can be observed in Fig. 17, there are some zones in the region of interest which should be avoided by the vehicles, as the environmental obstacles. In addition, it is mentioned in [25] that the emitters are detected whenever they are in the range of $1km$ of the vehicle's sensor.

The result of the detection procedure is stated in Table II. As can be observed, the eight emitters are detected by the method of [25] in $333.33s$, while our proposed algorithm leads to detection of these emitters in $181.12s$.

As the second similar work, [26] is considered, where the flying-vehicles are equipped with RSSI sensors, and aim to detect and localize the emitters. In each vehicle, a Mont Carlo filter is implemented to fuse its measurements with other vehicles' measurements. Then, the guidance points are generated, and the searching guidance law directs the vehicle through these points.

The region of interest is $40km \times 40km$ with the adjacent nodes' distance of $380m$. The number of neighboring vehicles searching for the emitters, varies from one to five, in separate scenarios. In each scenario, three parameters are investigated:

- detection time,
- success rate,
- income, which is defined as below ([26]).

$$In = n_t 10000 e^{\frac{-(D_t)^2}{400}} + 500 - n_s \frac{D_t}{60} 1500(\$), \qquad (30)$$

where n_t and n_s, are the number of localized emitters and flying-vehicles, respectively, and D_t is the detection time in minutes. The income value is larger for a mission with more detected emitters, fewer number of employed vehicles, and less hiring time.

The detection process of [26] is such that an emitter is declared detected whenever the vehicle gets as close as $50m$ to it. In the first scenario, one emitter is positioned at $(37,20)km$. The results are shown in Table III, where we can see that

- Both search algorithms lead to the detection of the emitter with 100% of success rate.
- Our proposed algorithm overcomes the algorithm of [26] from the detection time point of view. Also, it is observed that the cooperation of the vehicles plays a key role in the detection time parameter, as increasing the number of vehicles significantly improves this parameter.
- Our proposed algorithm results in better income values with respect to the Mont Carlo filtering method.

It is noteworthy that, as the authors have mentioned in [26], the method is best appropriate for one emitter. However, they have presented the outcome for detection of two emitters (positioned at $(35.1,16.2)km$,$(37,25.7)km$). The resulting success rate for the Mont Carlo Method and our proposed algorithm is shown in Table IV. As can be observed, while the Mont Carlo method is poor in this case, our proposed method leads to perfect detection.

In overall, the results represent the flexibility of the proposed algorithm with respect to various scenarios with different number of emitters, different number of vehicles, different step sizes, different nodes' distances, and, in general, different circumstances of the mission. Notably, in the proposed algorithm, when there is no signal in the environment, a suitable procedure (environmental unawareness criterion) is designed to look for possible targets. Then, a proper process (emitter likelihood criterion) is developed for the case of sensing signal from targets. These two logics together result in well detection of covert targets, while monitoring all intended zones of the surveillance region at the same time. Finally, an appropriate estimation procedure is used to track the detected targets, which completes the surveillance mission perfectly.

4 Complexity discussion

It can be inferred from the proposed surveillance scheme that its computational burden is directly related to the cost function defined in Equation (18). Indeed, without using the genetic algorithm, and through an exhaustive search to find the optimum solution, the total number of times, that the cost function should be computed[‡], is obtained from:

$$C_1 = \left(8 \times (8-1)^{K-1}\right)^{N_{\mathrm{V}}} P(N_{\mathrm{V}}, N_T), \qquad (31)$$

where 8 is the number of grid points surrounding around each grid point in our model, so that a vehicle have 8 choices to go at each step. In addition, P denotes permutation and other parameters are defined before. In this relation, the first term is the number of states due to the different paths that the vehicles can pass, and the second term is the different number of choices for assigning the search and track tasks to the vehicles.

On the other hand, for each time the cost function is computed, the computational burden is equal to:

[‡]which is in fact the total number of candidate solutions.

$$C_2 = F_S(K.\rho N_{\mathrm{V}}) + F_T(K.(1-\rho)N_{\mathrm{V}}) \propto N_{\mathrm{V}}, \tag{32}$$

where F_S is the time complexity of the search term of the cost function, and F_T is the time complexity of the track term of the cost function. ρ is the proportion of search vehicles to the overall number. Namely, Equation (32) is referred to as the *order of evaluate*.

The total complexity order of the aforementioned exhaustive search is obtained from the multiplication of two values of Equation (31) and Equation (32):

$$C_T = \left(8 \times 7^{K-1}\right)^{N_{\mathrm{V}}} N_{\mathrm{V}} P(N_{\mathrm{V}}, N_T) K \left(F_S \rho + F_T(1-\rho)\right). \tag{33}$$

Therefore, the complexity of an exhaustive search would grow in an exponential regime with respect to the number of vehicles, rather than polynomial.

It is shown that, by employing the genetic algorithm, the complexity would be on the order of $(C_2 \times m \ln m / \ln r)$ [27], where m is the population size and r is the fitness ratio[§]. Both of m and r are constants [27]. So, using Equation (32), the complexity order of the proposed genetic-based surveillance scheme will be $O(N_{\mathrm{V}})$. Therefore, it is observed that the exponential relation is reduced to a polynomial one, which leads to a much more efficient algorithm.

5 Conclusion

The problem of detection and tracking of stationary and moving emitters by multiple flying-vehicles, working in a cooperative manner, can be considered in any scenario, in which finding and monitoring a specific kind of radio emission source is desired. This may involve a vast range of applications, such as rescue, animal monitoring or localizing hostile radio equipment, etc. In this study, with the intention of using low-cost applicable agents, the flying-vehicles are considered to be equipped with only range sensors that measure the distance from radio emitters. In this case, in addition to detecting, the problem of localizing the emitters also arises. Moreover, the region of interest may consist of various obstacles which barricade the line of sight and therefore, add complexity to the surveillance.

It is shown that by introducing a suitable cost function combined with taking advantages of genetic algorithm, the routes and tasks of the vehicles can be obtained efficiently. This efficiency is based on three points of views: the complexity burden of solution, detection of new emitters, and track of detected emitters.

The proposed procedure is appropriate for various search and tracking missions where the primary solution is costly, irregular, or time inefficient. All these advantages are provided through an intelligent cooperation of agents.

Although the vehicles are considered to be equipped by range sensors, however, the proposed surveillance methodology can be easily adapted for employing the other radio sensors such as DF[¶]. Also, extending the proposed algorithm to the 3D (3-dimensional) can be considered as a future work, where the vehicles can change their height during the mission. All concepts presented in this paper in defining the proposed criteria are applicable to the 3D case, too. However, new gridding network should be defined and, probably, innovative approaches should be developed to overcome the computational issue of 3D scenarios. In addition to these subjects, considering the surveillance problem of cooperative vehicles with no prior knowledge of the terrain and moving towards more analytic methods while benefiting more advanced tracking filters would be interesting for future study.

[§]In more details, r can be referred to as the ratio of the average cost function value when setting a gene to 1, to the average cost value when setting that gene to 0. Obviously, this value is defined cost function dependent.

References

[1] Zhang, H., Xin, B., Dou, L., and et al., "A review of cooperative path planning of an unmanned aerial vehicle group," *Frontiers of Information Technology & Electronic Engineering*, 2020.

[2] Sargolzaei, A., Abbaspour, A., and Crane, C., "Control of cooperative unmanned aerial vehicles: review of applications, challenges, and algorithms," *Optimization, Learning, and Control for Interdependent Complex Networks*, 2020.

[3] Alotaibi, E., Alqefari, S., and Koubaa, A., "Lsar: Multi-uav collaboration for search and rescue missions," *IEEE Access*, Vol. 7, 2019.

[4] Scherer, J., Yahyanejad, S., Hayat, S., and et al., "An autonomous multi-UAV system for search and rescue," *Proceedings of the First Workshop on Micro Aerial Vehicle Networks, Systems, and Applications for Civilian Use*, 2015.

[5] Minaeian, S., Liu, J., and Son, Y., "Vision-based target detection and localization via a team of cooperative UAV and UGVs," *IEEE Transactions on systems, man, and cybernetics: systems*, Vol. 46, No. 7, 2015.

[6] Capitan, J., Merino, L., and Ollero, A., "Cooperative decision-making under uncertainties for multi-target surveillance with multiples UAVs," *Journal of Intelligent & Robotic Systems*, Vol. 84, 2016.

[7] Shaferman, V. and Shima, T., "Tracking multiple ground targets in urban environments using cooperating unmanned aerial vehicles," *Journal of Dynamic Systems, Measurement, and Control*, Vol. 137, No. 5, 2015.

[8] Xia, C., Yongtai, L., Liyuan, Y., and et al., "Cooperative Task Assignment and Track Planning For Multi-UAV Attack Mobile Targets," *Journal of Intelligent & Robotic Systems*, 2020.

[9] Mainwaring, A., Culler, D., Polastre, J., and et al., "Wireless sensor networks for habitat monitoring," *ACM international workshop on Wireless sensor networks and applications*, 2002.

[10] Hirsch, M. and Schroeder, D., "Dynamic decentralized cooperative control of multiple autonomous vehicles with multiple tasks for urban operations," *AIAA Guidance, Navigation, and Control Conference*, 2012.

[11] Nobahari, H., Effati, M., and Motie, M., "Cooperative search and localization of ground moving targets by a group of UAVs considering fuel constraint," *Scientia Iranica*, 2019.

[12] Pitre, R., Li, X., and Delbalzo, R., "UAV route planning for joint search and track missions—An information-value approach," *IEEE Transactions on Aerospace and Electronic Systems*, Vol. 48, No. 3, 2012.

[13] Saghafi, F. and Esmailifar, S. M., "Searching and localizing a radio target by an unmanned flying vehicle using bootstrap filtering," *Journal of Dynamic Systems, Measurement, and Control*, Vol. 137, No. 2, 2015.

[14] Esmailifar, S. M. and Saghafi, F., "Moving target localization by cooperation of multiple flying vehicles," *IEEE Transactions on Aerospace and Electronic Systems*, Vol. 51, No. 1, 2015.

[15] Riehl, J., Collins, G., and Hespanha, J., "Cooperative search by UAV teams: A model predictive approach using dynamic graphs," *IEEE Transactions on Aerospace and Electronic Systems*, Vol. 47, No. 4, 2011.

[16] Bansal, S., Goel, R., and Maini, R., "Ground vehicle and UAV collaborative routing and scheduling for humanitarian logistics using random walk based ant colony optimization," *Scientia Iranica*, 2022.

[17] Fang, S., O'Young, S., and Rolland, L., "Online Risk-based Supervisory Maneuvering Guidance for Small UAS Detect-and-Avoid Systems," *AIAA Journal of Guidance, Control, and Dynamics*, Vol. 11, 2017.

[18] Skolnik, M. I., "Radar handbook," 2008.

[19] Bernardo, J. and Smith, A., *Bayesian theory*, John Wiley & Sons, 2009.

[¶]Direction Finding

[20] Saho, K. and Masugi, M., "Performance analysis of α-β-γ tracking filters using position and velocity measurements," *EURASIP Journal on Advances in Signal Processing*, 2015.
[21] Mayiatis, D., "Comparison of an alpha-beta and kalman filter in track while scan radars," Tech. rep., Naval Postgraduate School Monterey, 1979.
[22] Daum, F., "Nonlinear filters: beyond the Kalman filter," *IEEE Aerospace and Electronic Systems Magazine*, Vol. 20, No. 8, 2005.
[23] Anderson, J., *Aircraft performance and design*, 1999.
[24] Tang, K., Man, K., Kwong, S., and et al., "Genetic algorithms and their applications," *IEEE Signal Processing Magazine*, Vol. 13, No. 6, 1996.
[25] Zhen, Z., Xing, D., and Gao, C., "Cooperative search-attack mission planning for multi-UAV based on intelligent self-organized algorithm," *Aerospace Science and Technology*, Vol. 76, 2018.
[26] Esmailifar, S. M. and Saghafi, F., "Cooperative localization of marine targets by UAVs," *Mechanical Systems and Signal Processing*, Vol. 87, 2017.
[27] Ankenbrandt, C., "An extension to the theory of convergence and a proof of the time complexity of genetic algorithms," *Foundations of genetic algorithms*, Elsevier, 1991.

Samine Karimi has received her B.Sc. and M.Sc. from Sharif University of Technology with the exceptional talented rank, respectively. She is currently pursuing the Ph.D. degree from the same university. Her research interests include Cooperative Missions, Guidance and Control, and Optimization.

Fariborz Saghafi has received his Ph.D in flight dynamics from Cranfield University, UK, in 1996. He is currently an associate professor in the Flight Dynamics and Control Group, Department of Aerospace Engineering, Sharif University of Technology. His interests include Flight Dynamics, Modeling and Simulation of Aerospace Systems, Aerial Robotics, Cooperative Missions, Rotorcraft, Simulator-Based Research and Education, Vision-Aided Navigation and Guidance, Aviation Industry.

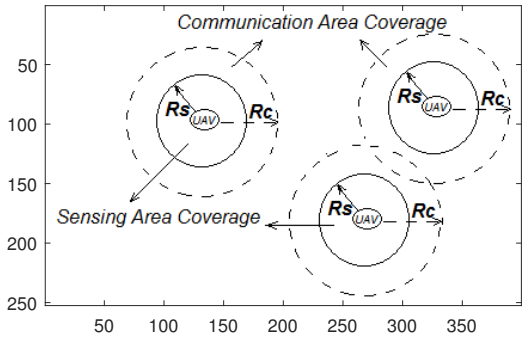

Fig. 1: Vechicles' network.

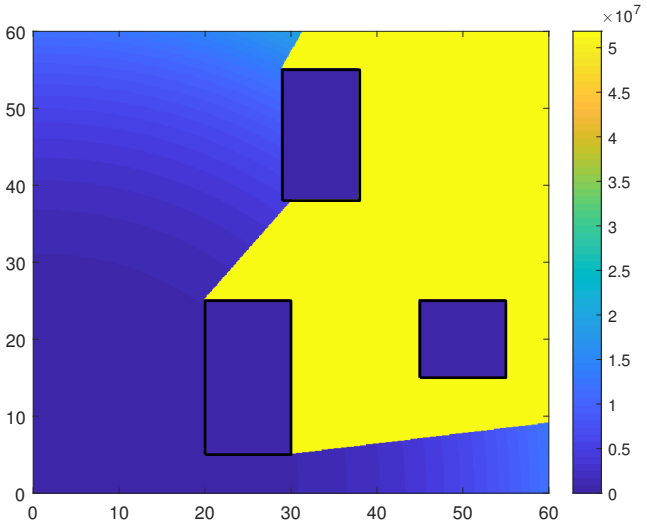

Fig. 2: A sample of region's unawareness level from a receiver point of view at $(0, 0)$.

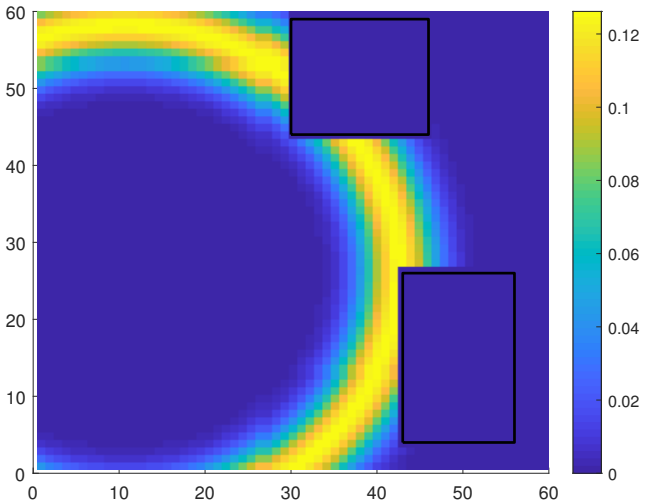

Fig. 3: A sample of emitter likelihood pattern for a vehicle at $(10, 25)$, which has sensed a signal with information of $d = 31.6m$.

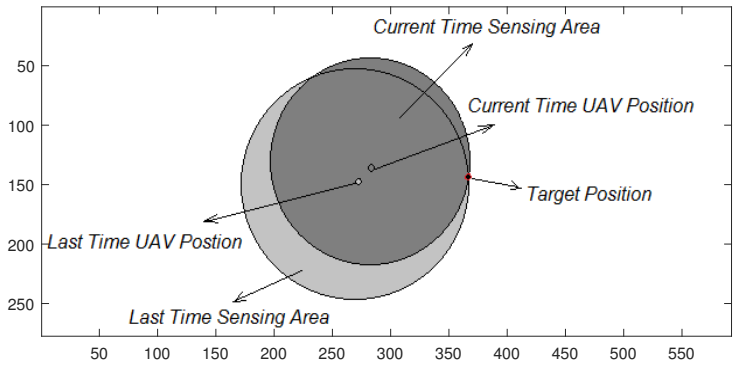

Fig. 4: Estimating the emitter's position by two successive range sensing.

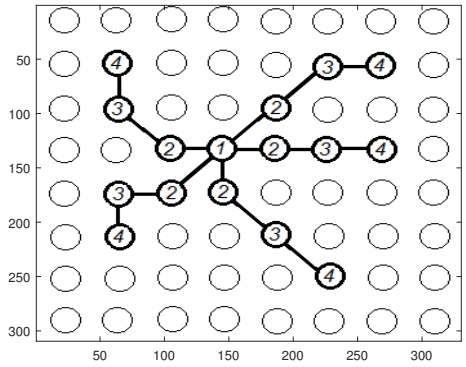

Fig. 5: Five candidate feasible routes.

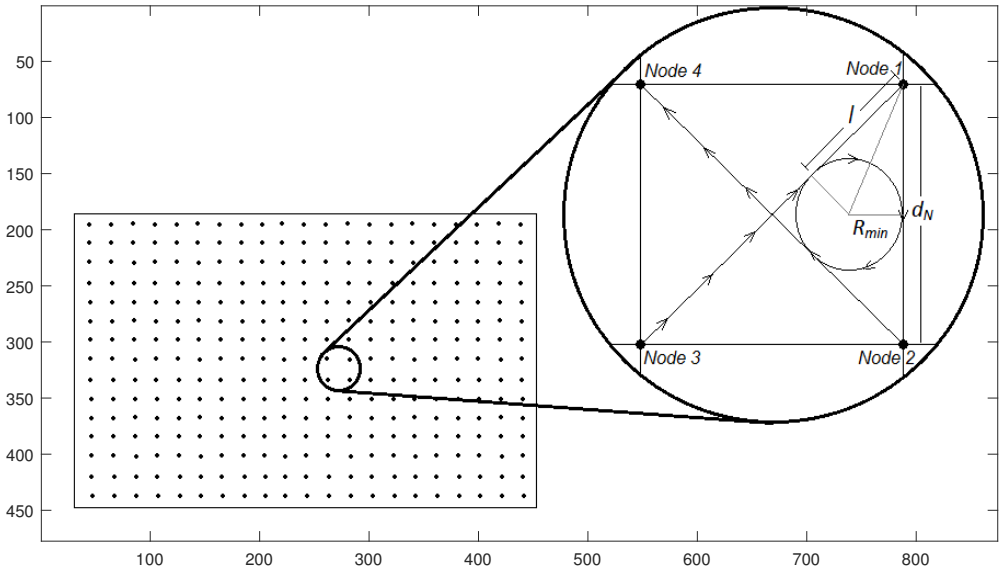

Fig. 6: Distance between two nodes and its relation with minimum turn radius.

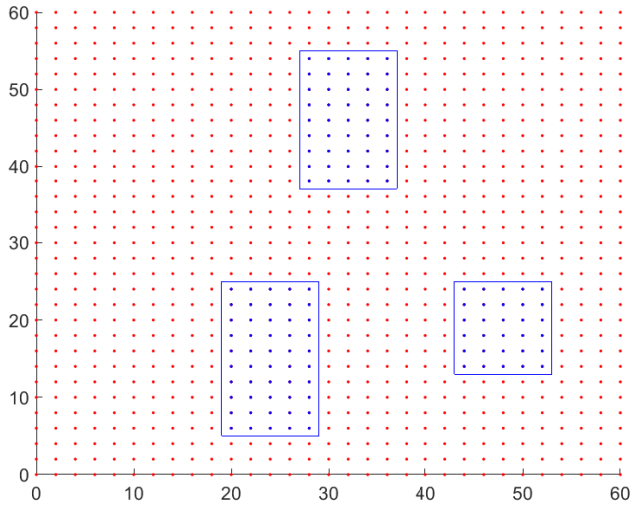

Fig. 7: The nodes inside the obstacles' boundaries (shown in blue) are not considered for producing candidate routes.

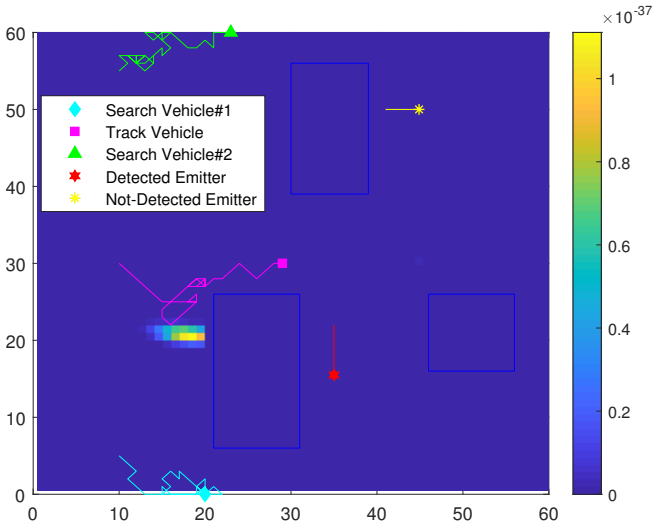

Fig. 8: Joint likelihood function for the 14'th optimization.

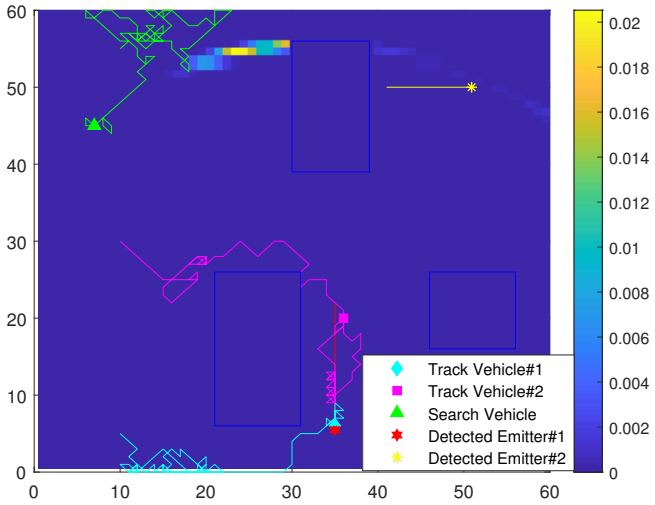

Fig. 9: Joint likelihood function for the 34'th optimization.

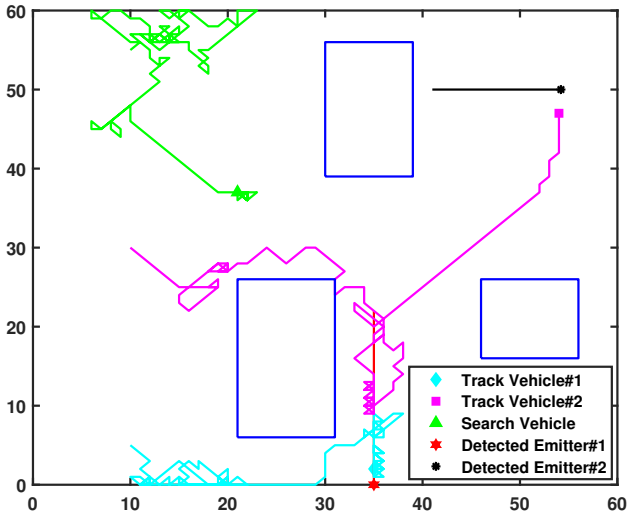

Fig. 10: The overall vehicles' trajectories.

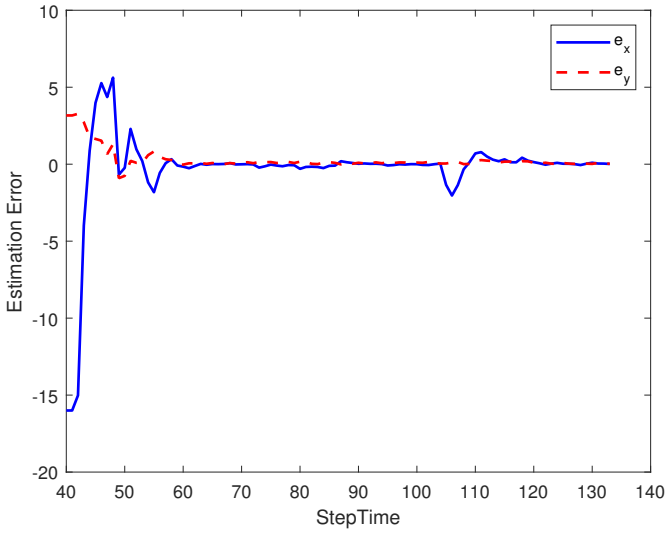

Fig. 11: Position estimation error of the first emitter.

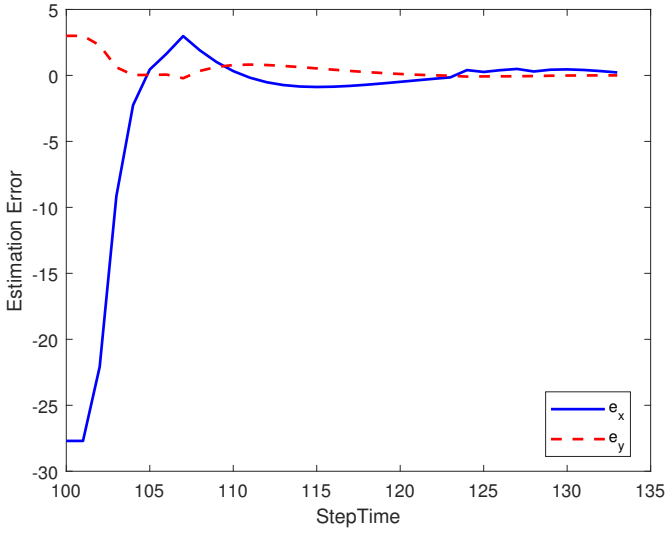

Fig. 12: Position estimation error of the second emitter.

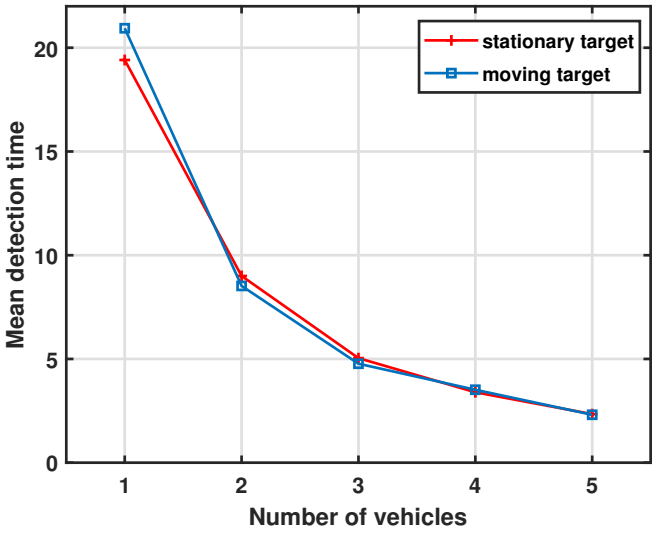

Fig. 13: Effect of cooperation on detection time.

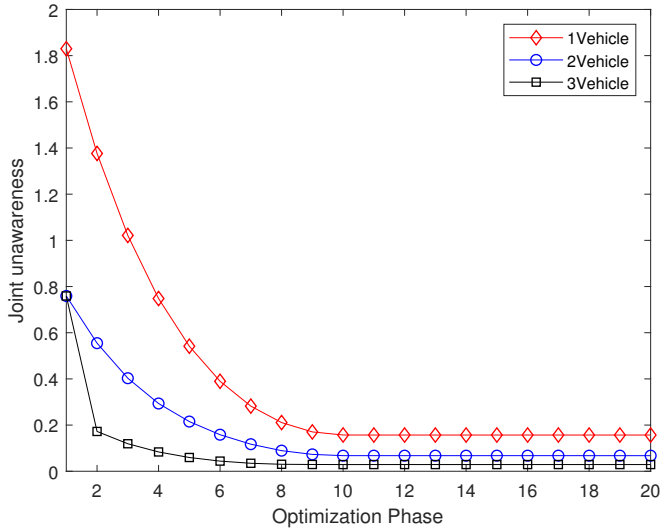

Fig. 14: Joint unawareness level.

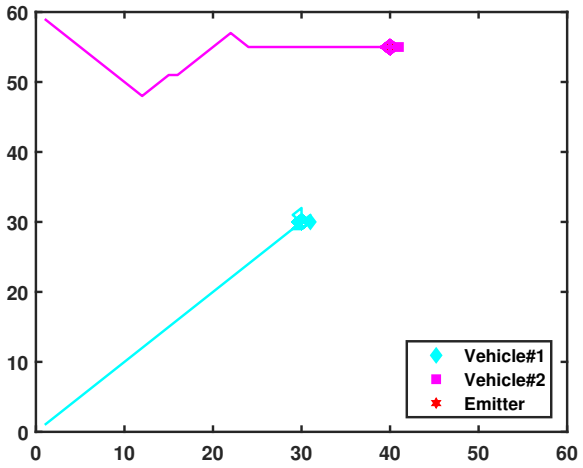

(a) $V = 0$

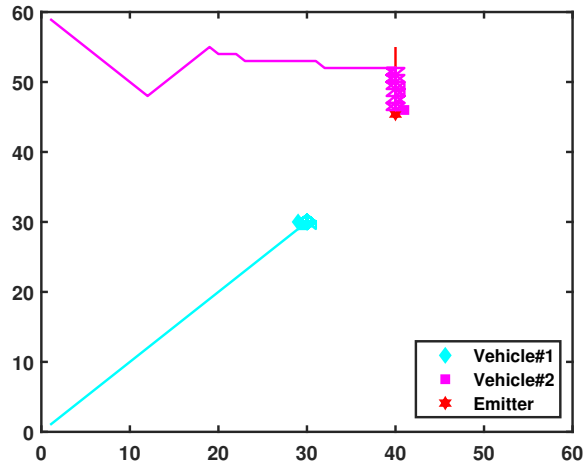

(b) $V = 10.36km/h$

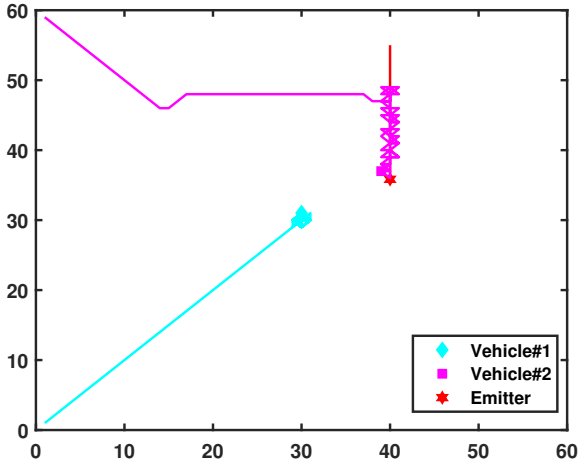

(c) $V = 20.73km/h$

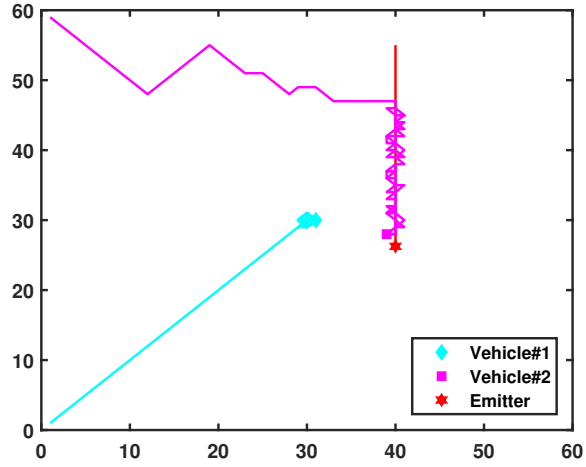

(d) $V = 31.10km/h$

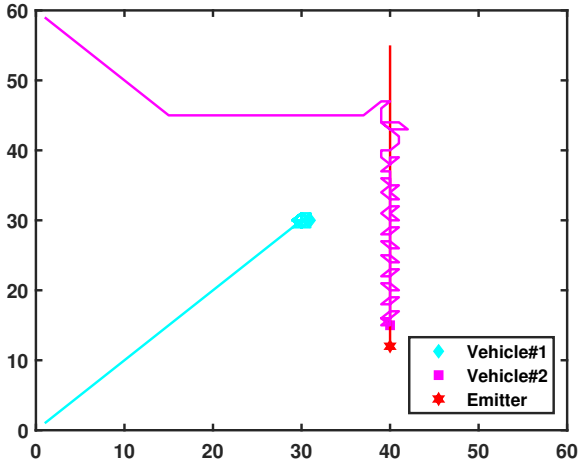

(e) $V = 41.45km/h$

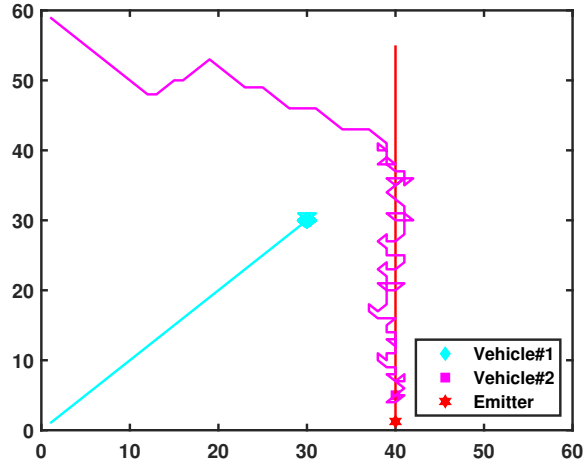

(f) $V = 51.82km/h$

Fig. 15: Vehicles' trajectories.

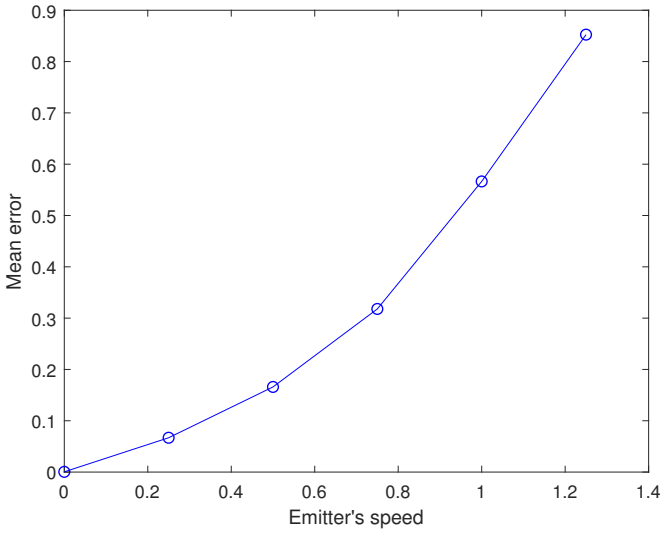

Fig. 16: Mean error of the emitter's position estimation.

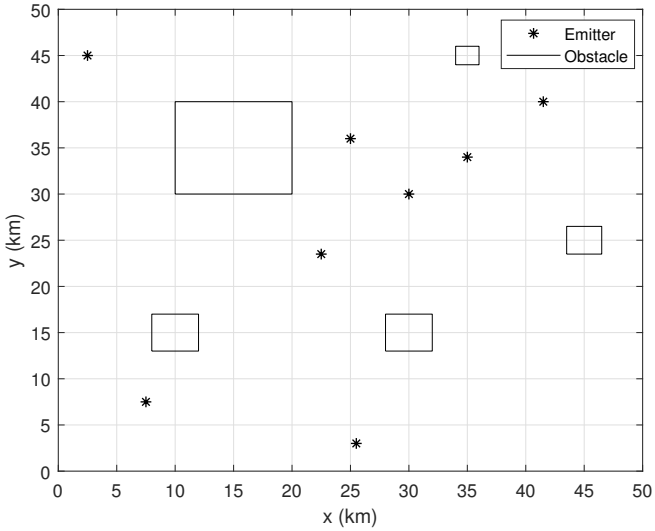

Fig. 17: Scenario of detection in [25]

TABLE I: Scenarios for different emitter's velocities

Scenario	Normalized velocity vector	Speed (km/h)
1	$(0;0)$	0
2	$(0;-0.083)$	10.36
3	$(0;-0.167)$	20.73
4	$(0;-0.250)$	31.10
5	$(0;-0.333)$	41.45
6	$(0;-0.417)$	51.82

TABLE II: Detection time in the presence of obstacles (s)

	ACO method of [25]	proposed method
Detection time	333.33	181.12

TABLE III: Performance evaluation according to criteria introduced in [26]

	Mean detection time (s)		Success rate (%)		Income value	
Number of vehicles	Method of [26]	Proposed method	Method of [26]	Proposed method	Method of [26]	Proposed method
1	1619	818.07	100	100	3014	6442
2	831	193.05	100	100	5953	10084
3	749	151.8	100	100	6167	10152
4	714	152.13	100	100	6118	10087
5	685	89.1	100	100	6029	10259

TABLE IV: Performance evaluation with two emitters

	Success rate in detection of two emitters (%)	
Number of vehicles	Method of [26]	Proposed method
1	8	100
2	42	100
3	52	100
4	64	100
5	62	100